Quantification of sediment-water interactions in a polluted tropical river through biogeochemical modeling

Anh Duc Trinh,[1] Filip Meysman,[2] Emma Rochelle-Newall,[3] and Marie Paule Bonnet[4]

Received 27 September 2010; revised 30 May 2012; accepted 15 June 2012; published 3 August 2012.

[1] Diagenetic modeling presents an interesting and robust way to understand sediment–water column processes. Here we present the application of such a model to the Day River in Northern Vietnam, a system that is subject to high levels of domestic wastewater inputs from the Hanoi metropolitan area. Experimental data from three areas of different water and sediment quality, combined with some additional data from the river, are used to set up and calibrate a diagenetic model. The model was used to determine the role of the sediments as a sink for carbon and nutrients and shows that in the dry season, 27% of nitrogen, 25% of carbon, and 38% of phosphorus inputs into the river system are stored in sediments. The corresponding numbers during the rainy season are 15%, 10%, and 20%, respectively. The diagenetic model was then used to test the impact of an improvement in the treatment of Hanoi's municipal wastewater. We show that improved wastewater treatment could reduce by about 17.5% the load of organic matter to the sediment. These results are the first to highlight the importance of sediments as a potential removal mechanism of organic matter and nutrients from the water column in this type of highly impacted tropical urban river, further demonstrating that rivers need to be considered as reaction sites and not just as inert conduits.

Citation: Trinh, A. D., F. Meysman, E. Rochelle-Newall, and M. P. Bonnet (2012), Quantification of sediment-water interactions in a polluted tropical river through biogeochemical modeling, *Global Biogeochem. Cycles*, *26*, GB3010, doi:10.1029/2010GB003963.

1. Introduction

[2] Many of the rivers that have their source in the Himalayas and on the Tibetan Plateau carry heavy sediment and nutrient loads, often resulting in large, highly productive, alluvial floodplains [*Winemiller et al.*, 2008]. These Asian river basins are also characterized by rapidly growing populations, shifts in land use, intensification of agricultural practices and increasing industrialization and urbanization. All of these factors have led to changes in natural flow regimes and deteriorating water quality [e.g., *Dudgeon*, 2000; *Pringle et al.*, 2000; *Wishart et al.*, 2000].

[3] As pointed out by *Cole et al.* [2007], river systems are more than just pipelines via which water and organic matter is transferred from the terrestrial environment to the coastal system. Globally, it is estimated that about 40% of the terrestrial carbon arriving in freshwater systems is returned to the atmosphere as CO_2 and a further 12% is buried in the sediments, with only 48% of the terrestrial carbon input reaching the coastal seas. These are global estimates and the determination of latitudinal differences is hampered by the paucity of studies in tropical systems, particularly in South East Asia. Only a limited number of studies on river biogeochemical functioning have been published in this region, addressing different aspects such as aqueous chemistry [*Lewis*, 2008], primary production [*Davies et al.*, 2008], and ecology [*Boulton et al.*, 2008; *Jacobsen et al.*, 2008]. However, up until now, few studies have investigated the impact of sedimentary processes on water quality.

[4] South East Asian rivers are characterized by a combination of high temperatures, excessive alluvial deposition, and untreated wastewater inputs. Therefore, it is likely that sedimentary processes play a crucial role in biogeochemical cycling in these rivers, potentially controlling nutrient availability and water quality. Despite the biogeochemical importance of sediments, the interactions between them and the overlying river water is poorly documented in tropical climates. Consequently, more detailed investigations into the biogeochemical cycling in South East Asian river systems are needed, both for management purposes as well as to better understand the anthropogenic effects on C, N, and P cycles.

[5] Here we present field observations and the associated modeling results of sediment-water interactions in the Day

[1]Laboratory of Analytical Science, Institute of Chemistry, Vietnam Academy of Science and Technology, Hanoi, Vietnam.
[2]Royal Netherlands Institute of Sea Research, Yerseke, Netherlands.
[3]Laboratory of Biogeochemistry and Ecology of Continental Ecosystems, UMR 7618-IRD, Ecole Normale Supérieure, Paris, France.
[4]Laboratory of Mechanics and Transfer in Geology, UMR 5563–IRD–Observatory Midi-Pyrénées, Université Paul Sabatier-Toulouse III, Toulouse, France.

Corresponding author: A. D. Trinh, Laboratory of Analytical Science, Institute of Chemistry, Vietnam Academy of Science and Technology, A18, 18 Hoang Quoc Viet Str., Hanoi, Vietnam. (ducta@ich.vast.ac.vn; trinhanhduc@yahoo.com)

0886-6236/12/2010GB003963

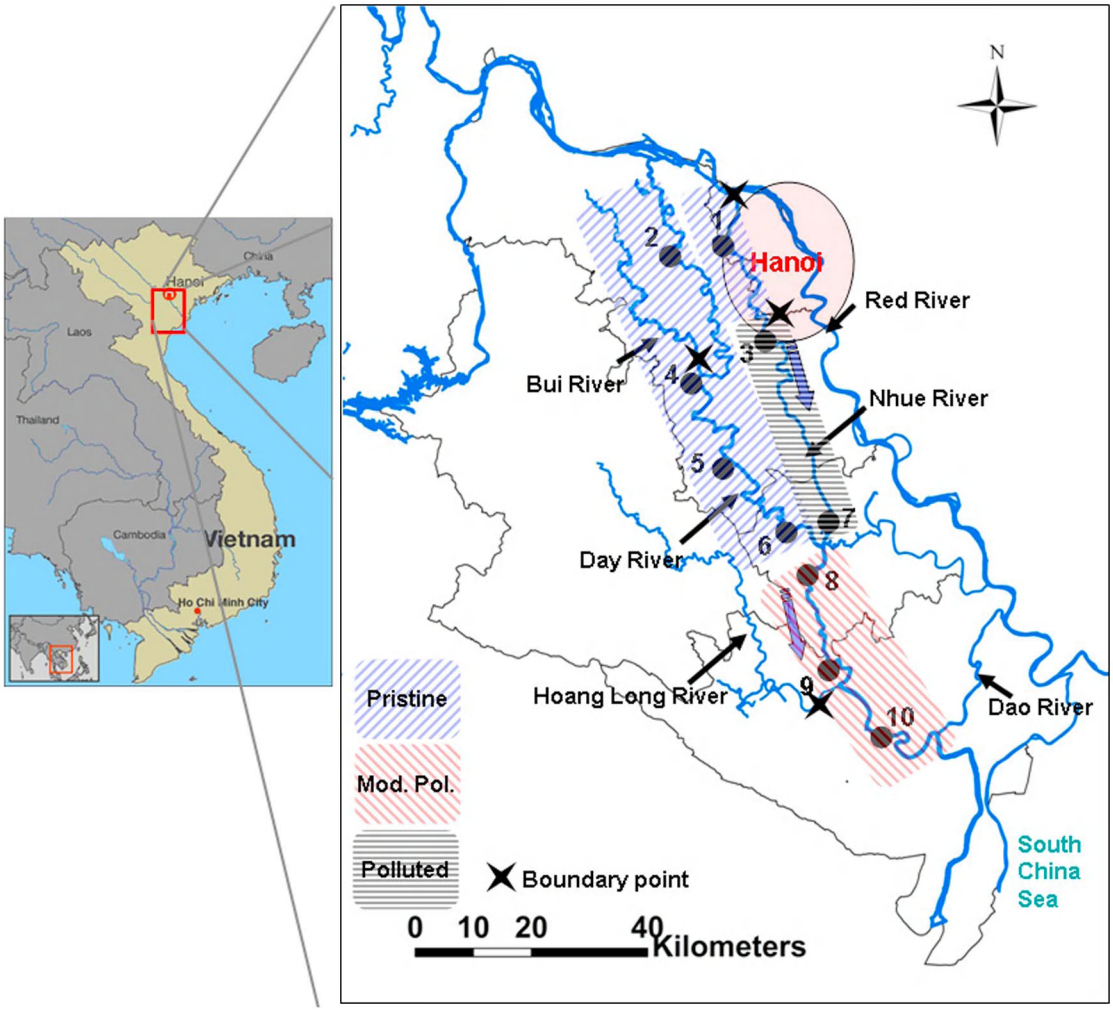

Figure 1. Map of the Nhue-Day basin and locations of experimental points (black dots). The latitude and longitude of the points and their location within the three zones is given in Table 1.

River, part of the Red River system, Northern Vietnam. The Day River flows through the lowland, metropolitan area of Hanoi and is subject to high levels of untreated wastewater inputs [*Trinh et al.*, 2009], and thus faces the same environmental issues as many other South East Asian river systems. The goals of this study were to quantitatively assess the importance of sediments in governing the overlying water quality and to provide carbon and nutrient (N and P) budgets for the Day River catchment.

2. Materials and Methods

2.1. Study Area and Selection of Sampling Sites

[6] The study area is located in the upstream part of the Day River basin (Red River delta, Northern Vietnam) with the studied area covering approximately 1920 km^2 (Figure 1). This basin is densely populated with a total population of more than 10.2 million, and drains the capital of Vietnam, Hanoi (6.5 million inhabitants) (General Statistics Office of Vietnam, 2010, http://www.gso.gov.vn/default_en.aspx?tabid=387&idmin=3&ItemID=11505). Historically, the Day River was part of the larger Red River network, but is now virtually isolated from the Red River due to a sluice lock built in the early 20th century. Today, the Day River receives its water from three main tributaries—the Bui, Hoang Long, and Nhue rivers (Figure 1). The Bui and Hoang Long rivers drain a mountainous region, whose hydrology and water quality are relatively less impacted by human activities. In contrast, the hydrological regime of the Nhue River is strongly controlled by irrigation as well as receiving most of the untreated domestic and industrial wastewater from the Hanoi metropolitan area [*Trinh et al.*, 2007].

[7] The Day River basin has a mean annual rainfall of 1860 mm yr^{-1}, of which 85% occurs from May to October (rainy season). The mean annual evapotranspiration ($\sim$1010 mm yr^{-1}) is distributed homogeneously over the area, and represents approximately 60–70% of the annual rainfall. The discharge of the Day River and its right bank tributaries (Hoang Long and Bui rivers) follow the same seasonal trend as rainfall. In contrast, the discharge of the Nhue River is more constant, with sporadic peaks that are linked to the operation of the sluice lock connection with the

Table 1. Coordinates of Sampling Sites and Sampling Dates

Site	Zone	Latitude (North)	Longitude (East)	Date
1	Pristine	21°00′23.05″	105°45″45.90″	18 Jan 2005
2	Pristine	20°56′11.80″	105°43′37.02″	13 Mar 2007
3	Polluted	20°55′11.77″	105°47′21.69″	25 Jan 2005; 20 Aug 2007
4	Pristine	20°48′33.77″	105°42′32.79″	17Apr 2007
5	Pristine	20°41′13.34″	105°44′46.68″	17 Apr 2007
6	Pristine	20°34′28.88″	105°52′14.36″	15 May 2007
7	Polluted	20°33′48.65″	105°55′11.14″	1 Feb 2005; 20 Aug 2007
8	Moderately polluted	20°30′59.08″	105°54′39.83″	12 Apr 2006
9	Moderately polluted	20°21′47.52″	105°55′16.15″	26 Apr 2006
10	Moderately polluted	20°13′03.58″	106°02′42.16″	26 Apr 2006

Red River. The mean annual discharge of this upper part of the Day River system is 120 $m^3 s^{-1}$. The sediment load from this upper part to the estuarine area was estimated at approximately 410 ton d^{-1}. A more detailed description of the hydrology and sedimentation of the Day River system can be found in *Luu et al.* [2010, 2012].

[8] *Trinh et al.* [2009] recently showed that the section of the Day River close to the Hanoi downtown area is heavily polluted, while the zone upstream is relatively less polluted. These authors separated the Day River system into three different zones based on the degree of pollution: 1) a "pristine" upstream zone, 2) a heavily "polluted" central zone, and 3) the "moderately polluted" downstream zone (Figure 1). Based on this zonation, we selected 10 sampling stations distributed across the three zones (Figure 1). The geographical coordinates of the sampling locations and the sampling dates are provided in Table 1. In fact, this study is part of a larger environmental research project started in 2000 on the Nhue-Day River system, the main focus of which is to investigate the anthropogenic impacts on water quality [*Trinh et al.*, 2009; *Luu et al.*, 2010; *Le et al.*, 2010; *Duong et al.*, 2012]. During the period of this study, the water quality and hydrology of the Nhue River system were regularly surveyed and these additional data were combined with the current data set on sediment biogeochemistry to produce a basin-scale budget for C, N, and P.

2.2. Sediment Collection

[9] Sediment cores were collected using polycarbonate tubes (10 cm i.d.) from 1.5 m water depth. At each site, 3 cores were collected within a distance of 1 m, each time retrieving approximately 20 cm of sediment. Cores were immediately sealed and transferred to the laboratory at 4°C. Upon return to the laboratory, sediment cores were extruded and sliced in an N_2 filled glove bag. Subsamples of 1 cm thick slices were collected from depths of 0, 2, 4, 6, 10, 15, and 20 cm of the cores. The corresponding depth slices of the three replicate cores from each site were combined and homogenized. Pore water was extracted by centrifugation for 30 min at 5000 rpm under an N_2 atmosphere using a Heraeus Multifuge 3SR. Samples were then filtered using 0.45 μm cellulose filter membranes for analysis of total alkalinity (Alk), ammonium (NH_4^+), nitrate (NO_3^-), soluble reactive phosphate (PO_4^{3-}), and total dissolved iron (Fe) and manganese (Mn). Separate sediment samples were dried and stored for elemental analyses of porosity, organic carbon (Corg), total nitrogen (N_{tot}), total phosphorus (Ptot), total Fe (Fe_{tot}), and total Mn (Mn_{tot}).

2.3. Chemical Analysis

[10] Concentrations of Alk, NH_4^+, NO_3^-, and PO_4^{3-} in pore water were determined according to the Standard methods for the examination of water and wastewater [*Clesceri et al.*, 1999]. Total alkalinity was determined by a fixed end point titration with 0.1 N HCl using methyl orange as an indicator (Standard method 2320 in *Clesceri et al.* [1999]). It should however be noted that this method is less accurate under anoxic conditions due to the interference of hydrogen sulphides and other anions during titration. Nitrate was determined by quantitative reduction to nitrite on a cadmium column, followed by colorimetric determination at 540 nm of the nitrite using the Griess reaction (Standard method 4500-NO_3 E in *Clesceri et al.* [1999]). Ammonium (NH_4^+) was determined colorimetrically at 640 nm by the phenolhypochlorite method (Standard method 4500-NH3 F. phenate in *Clesceri et al.* [1999]). Soluble reactive phosphate concentrations were determined colorimetrically at 880 nm by the ascorbic acid method (Standard method 4500-P E in *Clesceri et al.* [1999]). All colorimetric measurements were conducted on a GBC Cintra 40 spectrophotometer (Australia).

[11] Porosity, organic matter (OM), total nitrogen (N_{tot}), total phosphorus (P_{tot}), total iron (Fe_{tot}) and total manganese (Mn_{tot}) were determined on centrifuged sediment samples. Sediment porosity was determined by weight difference after drying at 105°C for 6 h and calculated as described in *Lewandowski and Hupfer* [2005]. It should be noted that this method, although not precise as using porosimeters, is often used in this kind of study. Samples for sediment organic carbon content (C_{org}) were first acidified with a 2 N H_2SO_4 – 5% $FeSO_4$ solution to remove inorganic carbonates. Samples were then digested at 150°C for 30 min following the modified Walkley-Black procedure [*Walkley and Black*, 1934]. Total nitrogen (N_{tot}) was measured using the Total Kjeldahl Nitrogen (TKN) method (4500-N_{org} B) [*Clesceri et al.*, 1999]. Centrifuged sediment samples of 0.5 g were digested in concentrated H_2SO_4 catalyzed by K_2SO_4, $FeSO_4$, and $CuSO_4$ by the use of a Buchi K-435 digestion unit for 1 h at maximum temperature of 350°C. The sample was then distilled in a Buchi B-324 distillation unit, before titration with 0.1 N H_2SO_4 and boric acid (4%) as the indicator for N_{tot} content. Total Phosphorus (P_{tot}) was determined on 0.5 g samples by addition of concentrated $HClO_4$ solution at 150°C for 2 h followed by determination of PO_4^{3-} by the ascorbic acid method as detailed above. Total Fe and Mn were determined with an atomic absorption spectrometer (AAS) on a Perkin-Elmer 3300 instrument. One gram of

Table 2. Detailed Mathematical Formulation for Conversion Rates of the Diagenetic Model

Number	Processes	Conversion Rates/Kinetic Equation[a]
1	Mineralization with O_2	$k_{O_2,T^0} e^{\beta_{Oxic}(T-T^0)} \frac{C_{O_2}}{K_{O_2}+C_{O_2}} X_{Degr.}$
2	Mineralization with NO_3^-	$k_{NO_3,T^0} e^{\beta_{Anox}(T-T^0)} \frac{K_{O_2}}{K_{O_2}+C_{O_2}} \frac{C_{NO_3}}{K_{NO_3}+C_{NO_3}} X_{Degr.}$
3	Mineralization with Fe^{3+}	$k_{FeOOH,T^0} e^{\beta_{Anox}(T-T^0)} \frac{K_{O_2}}{K_{O_2}+C_{O_2}} \frac{K_{NO_3}}{K_{NO_3}+C_{NO_3}} \frac{X_{FeOOH}}{K_{FeOOH}+X_{FeOOH}} X_{Degr.}$
4	Mineralization with SO_4^{2-}	$k_{SO_4,T^0} e^{\beta_{Anox}(T-T^0)} \frac{K_{O_2}}{K_{O_2}+C_{O_2}} \frac{K_{NO_3}}{K_{NO_3}+C_{NO_3}} \frac{K_{FeOOH,inh}}{K_{FeOOH,inh}+X_{FeOOH}} \frac{C_{SO_4}}{K_{SO_4}+C_{SO_4}} X_{Degr.}$
5	Mineralization with CO_2	$k_{CO_2,T^0} e^{\beta_{Anox}(T-T^0)} \frac{K_{O_2}}{K_{O_2}+C_{O_2}} \frac{K_{NO_3}}{K_{NO_3}+C_{NO_3}} \frac{K_{FeOOH,inh}}{K_{FeOOH,inh}+X_{FeOOH}} \frac{K_{SO_4,inh}}{K_{SO_4,inh}+C_{SO_4}} X_{Degr.}$
6	$Fe + HS \Leftrightarrow FeS + H$	$k_{FeS,pre}\left(\frac{C_{Fe}C_{HS}K_{eq,S}}{C_H K_{eq,FeS}} - 1\right) C_{Fe}$ if $\frac{C_{Fe}C_{HS}K_{eq,S}}{C_H K_{eq,FeS}} > 1$
		$k_{FeS,diss}\left(1 - \frac{C_{Fe}C_{HS}K_{eq,S}}{C_H K_{eq,FeS}}\right) X_{FeS}$ if $\frac{C_{Fe}C_{HS}K_{eq,S}}{C_H K_{eq,FeS}} \le 1$
7	$3Fe + 2\,HPO_4 \Leftrightarrow Fe_3(PO_4)_2 + 2\,H$	$k_{Fe_3(Po_4)_2,pre}\left(\frac{C_{Fe}^3 C_{HPO_4}^2 K_{eq,PO_4}^2}{C_H^2 K_{eq,Fe_3(PO_4)_2}} - 1\right) C_{Fe}$ if $\frac{C_{Fe}^3 C_{HPO_4}^2 K_{eq,PO_4}^2}{C_H^2 K_{eq,Fe_3(PO_4)_2}} > 1$
		$k_{Fe_3(Po_4)_2,diss}\left(1 - \frac{C_{Fe}^3 C_{HPO_4}^2 K_{eq,PO_4}^2}{C_H^2 K_{eq,Fe_3(PO_4)_2}}\right) X_{Fe_3(Po_4)_2}$ if $\frac{C_{Fe}^3 C_{HPO_4}^2 K_{eq,PO_4}^2}{C_H^2 K_{eq,Fe_3(PO_4)_2}} \le 1$
8	$FeCO_3 + H \Leftrightarrow Fe + HCO_3$	$k_{Feco_3,pre}\left(\frac{C_{Fe}C_{HCO_3}K_{eq,CO_2}}{C_H K_{eq,FeCO_3}} - 1\right) C_{Fe}$ *if* $\frac{C_{Fe}C_{HCO_3}K_{eq,CO_2}}{C_H K_{eq,FeCO_3}} > 1$
		$k_{Feco_3,diss}\left(1 - \frac{C_{Fe}C_{HCO_3}K_{eq,CO_2}}{C_H K_{eq,FeCO_3}}\right) X_{FeCO_3}$ *if* $\frac{C_{Fe}C_{HCO_3}K_{eq,CO_2}}{C_H K_{eq,FeCO_3}} \le 1$
9	$CaCO_3 + H \Leftrightarrow Ca + HCO_3$	$k_{caco_3,pre}\left(\frac{C_{Ca}C_{HCO_3}K_{eq,CO_2}}{C_H K_{eq,CaCO_3}} - 1\right) C_{Ca}$ if $\frac{C_{Ca}C_{HCO_3}K_{eq,CO_2}}{C_H K_{eq,CaCO_3}} > 1$
		$k_{caco_3,diss}\left(1 - \frac{C_{Ca}C_{HCO_3}K_{eq,CO_2}}{C_H K_{eq,CaCO_3}}\right) X_{CaCO_3}$ if $\frac{C_{Ca}C_{HCO_3}K_{eq,CO_2}}{C_H K_{eq,CaCO_3}} \le 1$

[a]X denotes the concentration in solid phase.

sediment was added to 5 ml of concentrated $HNO_3 + HClO_4$ (1:1 volume equivalents) and digested in an Aurora MW500 microwave (Canada) for 30 min. After digestion, the volume of the sample was adjusted to 50 ml with purified water prior to AAS determination following the 3111 method presented in *Clesceri et al.* [1999].

2.4. Reactive Transport Modeling

[12] To simulate the degradation of organic matter and other geochemical processes in sediment column, a 1-D diagenetic model was developed.

2.4.1. Model Formulation

[13] The reactive transport model follows the standard formulation for early diagenetic models of aquatic sediments (CANDI [*Boudreau*, 1996]; OMEXDIA [*Soetaert et al.*, 1996]; STEADYSED [*Van Cappellen and Wang*, 1996]; MEDIA [*Meysman*, 2001]). The model simulates the depth profiles of solutes and solids, as well as the fluxes across the sediment-water interface, based on the mass balance equations

$$\frac{\partial(\phi C_S)}{\partial t} = \frac{\partial}{\partial z}\left[\phi D_S \frac{\partial C_S}{\partial z}\right] - \frac{\partial}{\partial z}[\phi \omega C_S] + \sum_i \nu_{S,i} R_i, \quad (1)$$

$$\frac{\partial([1-\phi]C_P)}{\partial t} = \frac{\partial}{\partial z}\left[[1-\phi] D_P \frac{\partial C_P}{\partial z}\right] - \frac{\partial}{\partial z}[[1-\phi]\omega C_P] + \sum_i \nu_{P,i} R_i, \quad (2)$$

where C_S and C_P are the concentration of the solute and solid species [M L^{-3}], respectively; t is time [T]; z is depth [L]; D_S and D_P are, respectively, the effective diffusion coefficients of solute and solid species [L^2 T^{-1}]; ω is the sedimentation velocity [L T^{-1}]; ϕ is porosity; R_i is the reaction rate due to biogeochemical processes [M L^{-3} T^{-1}]; and $\nu_{S,i}$ and $\nu_{P,i}$ are the stoichiometric coefficients of the solute and solid species in the *i*th reaction, respectively.

[14] There are two types of reaction in this model: 1) microbial degradation involving different redox pairs and 2) geochemical reactions (nonredox reactions). Reaction rates for degradation processes are expressed as

$$R_i = k \times \text{lim} \times \text{inh} \times C, \quad (3)$$

where C is the concentration of the component under study; k is the maximum degradation rate in optimal conditions [T^{-1}]; "lim" is the limitation function due to substrate availability; and "inh" is an inhibition term. Limitation functions follow the classical Michaelis-Menten relation

$$\text{lim} = \frac{C}{C + K_C}, \quad (4)$$

where K_c is the half-saturation constant expressed in the same unit as the component C. Inhibition functions follow the relationship

$$inh = \frac{K_{inh}}{C_j + K_{inh}}, \quad (5)$$

where K_{inh} is the half-saturation constant of the component C_j responsible for the inhibition of the considered process. When several components inhibit a process, the relevant inhibition functions are multiplied. On the other hand, the geochemical reactions have a formulation as

$$R_i = k \times (C - C_{eq}), \quad (6)$$

where C is the concentration of the component under study; C_{eq} is the concentration when chemical equilibrium is reached; and k [T^{-1}] is the kinetic constant. Equilibrium constants

Table 3. Average Values of Sediment Profiles

	C (mg/g)	N (mg/g)	P (mg/g)	Molar C:N:P	Fe (mg/g)	Mn (mg/g)
Polluted	52.10	3.92	1.72	78:5:1	28.06	0.471
Moderately polluted	44.93	2.90	1.28	91:5:1	40.75	0.710
Pristine	39.35	2.11	1.17	87:4:1	47.43	0.879
Red River delta soil	8.1[a]–30.9[b]	1[c]–2[b]	0.26[c]–1.6[d]	80:8:1	39.11	0.457
World soil				186:13:1[e]		

[a]*Khai* [2007].
[b]*Tue et al.* [2011].
[c]*Ha et al.* [2006].
[d]*Le et al.* [2010].
[e]*Cleveland and Liptzin* [2007].

required for computing C_{eq} are extracted from the literature [*Morel and Hering*, 1993]. Detailed mathematical formulations for all the processes are listed in Table 2.

[15] The organic matter pool consists of two fractions (degradable and refractory). Only the degradable fraction reacts within the time scale of the model, and this degradation occurs via a sequence of mineralization pathways. The rate expressions for these reactions follow the standard kinetic rate laws for organic matter mineralization in which electron acceptors are consumed according to the thermodynamic free energy yield [*Tromp et al.*, 1995; *Soetaert et al.*, 1996].

2.4.2. Boundary Conditions and Parameterization

[16] The concentration of solutes at the sediment-water interface is fixed to that of the overlying water, while a fixed flux is imposed for the solids. The boundary concentrations for each solute are calculated by averaging the water quality results of the 2007 monthly surveys for each zone. Settling rates of suspended sediment and solid species are taken from *Trinh et al.* [2006] and are similar to those observed in the adjacent rivers [*van den Bergh et al.*, 2007]. The proportions of degradable and refractory fractions are taken from previous experiments on OM degradation in the river water and from *Trinh et al.* [2006] stoichiometry of C, H, O, N, P, and S for both OM pools are defined based on our experimental results (Table 3) as well as from other similar work [*Dittrich et al.*, 2009]. These boundary conditions are shown in Table 4.

2.4.3. Numerical Model Solution

[17] A numerical solution procedure is implemented in the open source programming language R as fully detailed in *Soetaert and Meysman* [2011]. A reactive transport model essentially consists of one partial differential equation (PDE) for each compound. Following the method of lines, the R-package ReacTran uses a finite difference scheme to expand the spatial derivatives of the PDEs over the sediment grid. After finite differencing, the resulting set of ordinary differential equations (ODEs) is integrated using the stiff equation solver code from the R-package deSolve [*Soetaert et al.*, 2010].

2.4.4. Two-Step Model Construction Tactic

[18] Model development and calibration of early diagenesis are always a compromise between describing the system's complexity in detail and using a manageable set of reactions with known or calibrated parameters or variables [*Katsev et al.*, 2004]. In this study, a two-step tactic is implemented to reduce the constraints between the model complexity and parameter set and data availability. Initially, the model is compiled to include only the degradation of organic matter where the main oxidizers are selected based on their dominance in this river sediment. Then, simulation results of the initial modeling step are used in a series of geochemical computations to identify the most important geochemical reactions occurring at each considered sediment depth. All the experimental results are exploited in order to have the best compromise between data availability and model complexity.

2.5. Budget Calculation

[19] At present there are very few published nutrient or carbon budget calculations for the rivers in Northern Vietnam. *Quynh et al.* [2005] and *Le et al.* [2010] provide some estimates of sediment-water exchange in the lower part of the Red River basin by estimating retention using a stochastic approach. Storage in the river system was estimated as the difference between inputs from the catchment and outputs at the river mouth. In the deterministic approach presented here, "retention" is derived from the application of a diagenetic model that calculates organic carbon, nitrogen and phosphorus burial and the nutrient effluxes from the sediment in the studied river system.

[20] The C, N, and P mass balances for the Nhue-Day River system are then determined by combining the diagenetic modeling results obtained here with previous information on mass transport within the Nhue River [*Trinh et al.*, 2006, 2007] and from the data on tributarial inputs and

Table 4. Boundary Conditions Used in the Diagenetic Model and Additional Data Used for Budget Calculation

	Pristine	Moderately Polluted	Polluted
DIC (mol m^{-3})	2.01	2.15	3.11
O_2 (mol m^{-3})	0.1	0.07	0.04
NH_4 (mol m^{-3})	0.03	0.08	0.35
NO_3 (mol m^{-3})	0.034	0.029	0.021
SO_4 (mol m^{-3})	0.1	0.1	0.21
SRP (mol m^{-3})	0.006	0.007	0.024
Degradable OM (g m^{-2} d^{-1})	2.8	4.0	6.7
Refractory OM (g m^{-2} d^{-1})	3.0	3.0	4.0
Fe_{tot} (mol m^{-2} d^{-1})	0.045	0.045	0.045
Reducible Fe^{3+} (mol m^{-2} d^{-1})	0.147 × Fe_{tot}	0.147 × Fe_{tot}	0.147 × Fe_{tot}
Settling rate (cm yr^{-1})	5.35	6.33	8.76
Wetted area (dry season, km^2)	7.155	8.095	2.463
Wetted area (rainy season, km^2)	7.419	8.390	2.576

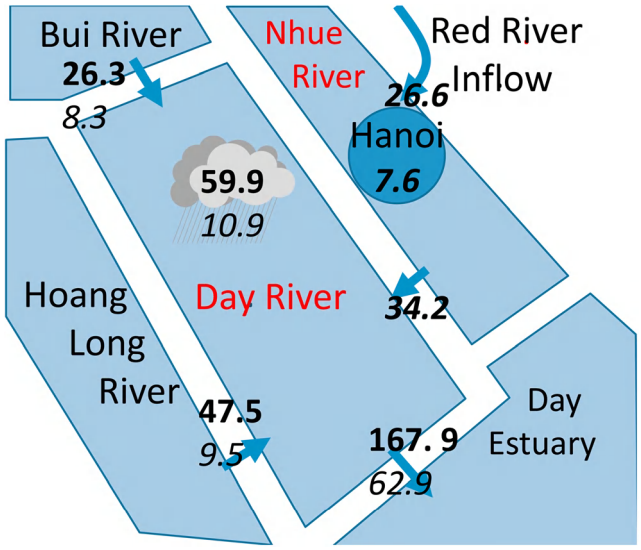

Figure 2. Hydrological network and water regime of the study area during the rainy season (bold) and dry season (italic). All values are in $m^3\ s^{-1}$.

lateral inflows from the Hanoi Metropolitan area to the Day River (Figure 2).

[21] Two scenarios are constructed for the budget calculation corresponding to the dry season and the rainy season. The difference between the two scenarios is that during the rainy season, the inflow from lateral sources and upstream tributaries is higher. Inflow from the Red River during both periods is set constant to reflect the fact that the flows from the Red River to the Nhue-Day River system (Figure 1) are well regulated by a complex system of dams and weirs.

[22] The budget calculation takes into account the whole river section of the Nhue River (74 km length), from its tightly controlled, sluice gate connection with the Red River to its confluence with the Day River and a 123 km reach of the Day River from its confluence with its upstream tributary —the Bui River—to the estuarine section. The estuarine section is defined from the Day River–Dao River confluence to the river mouth (Figure 1). Within this 123 km stretch, the Day River receives water from the catchment and water from the Nhue and Hoang Long Rivers, located at 66 km and 91.5 km, downstream of the confluence with the Bui River, respectively.

[23] The hydrological network and water regime are presented in Figure 2. Discharge is calculated from the rating curves of *Luu et al.* [2010] applied to daily water levels observed at gauging stations along the Nhue-Day River system in 2007 and lateral flow is taken from *Trinh et al.* [2006]. The calibration results of the hydrodynamic-biogeochemical river model applied to the Nhue River [*Trinh et al.*, 2006] were used to provide settling rates, the river perimeter and width and atmospheric-water exchange rate of CO_2 for the carbon budget calculation.

[24] Averaged water quality data obtained from our monthly surveys at boundary points and tributary inflow points during 2007 are used to calculate upstream loads [$M\ T^{-1}$]. The load [$M\ T^{-1}$] between water and sediment is calculated by multiplying exchange rate/flux [$M\ L^{-2}\ T^{-1}$] obtained from diagenetic modeling with wetted area [L^2]. The wetted area is calculated from river perimeter [L] and river length [L] (Table 4). The inflow OM at the boundary points is also separated into degradable and refractory fractions characterized by different C-N-P compositions. For simplicity, these compositions are taken to be identical to the corresponding values of OM deposited to the sediment (Table 5). The degradable:refractory ratio is extracted from the work of *Trinh et al.* [2006]; 0.89 for the water arriving from the tributaries and from upstream and 0.94 for water from the city of Hanoi.

[25] It should be noted that as residence time of sediment particle in a 20 cm sediment layer is several years. The layer thus integrates the changes between rainy and dry seasons. As the simulation corresponds to a converged steady state, the seasonal variability of diagenesis is considered minimal and therefore ignored in the diagenetic model. This means that the possible impact of extreme conditions such as storms, flooding events is not taken into account in the model.

3. Results and Discussion

3.1. Sediment Depth Profiles

3.1.1. Solid Species Profiles

[26] The organic matter content of the sediments was generally high and ranged between 4 and 6%. Significant differences are observed between the three zones (*t* test of paired data at confidence level of 0.05) with concentrations being highest in the polluted zone and lowest in the pristine zone (Figure 3). Overall, the organic carbon (C org), total Nitrogen (N tot), and total Phosphorus (P tot) are 4 to 6 times higher than typical values found in the fluvisols of the Northern Vietnam delta (Table 3) [*Ha et al.*, 2006; *Khai*, 2007]. Moreover, the carbon and nitrogen values for the polluted zone of the Day River subbasin are twice as high as the maximum values previously reported for riverine sediments in the Red River basin [*Tue et al.*, 2011; *Le et al.*, 2010].

[27] The organic carbon profiles are variable within the upper sediment layers, potentially reflecting the variable hydrological regime of the river. While N_{tot} and C_{org} decrease with depth, indicating organic matter degradation, P_{tot} profiles are generally constant with depth (Figure 3).

[28] Comparing the C:N:P ratios between the three zones, there is a slight decrease in the carbon content at the polluted sites as compared to the other two sites (Table 3). The soil of the Red River Delta has a similar C:P ratio but a higher N fraction than the Day River sediments. The low N content, relative to the soils, seems to prevail in the Red River sediments as *Tue et al.* [2011] also found C:N ratios as high as 18.32 at the Red River mouth. Denitrification may be one reason why there are lower N contents in the sediments. Comparison of the molar C:N:P ratio in this river system with the C:N:P in worldwide soil (Table 3) [*Cleveland and Liptzin*, 2007] clearly indicates very high fractions of N and P. Indeed, the ratios here are closer to those of microbial organisms than terrestrial plants [*Cleveland and Liptzin*, 2007]. Surprisingly, the total Fe content in the polluted sediment is much lower than in the pristine and the moderately polluted sediments. The high mobility of Fe in low-oxygen environments could provide an explanation for this. Over the 2005–2007 period of this study, the monthly surveys of the river surface water show an average Redox potential of

Table 5. Kinetic Parameters of the Diagenetic Model Processes

Symbol	Description	Value[a]	Unit
k_{O_2,T^0}	Max mineralization rate of organic matter with O_2 at 25°C	0.1	d^{-1}
k_{NO_3,T^0}	Max mineralization rate of organic matter with NO_3 at 25°C	0.08	d^{-1}
k_{FeOOH,T^0}	Max mineralization rate of organic matter with Fe^{3+} at 25°C	0.00003	d^{-1}
k_{SO_4,T^0}	Max mineralization rate of organic matter with SO_4 at 25°C	0.0008	d^{-1}
k_{CO_2,T^0}	Max mineralization rate of organic matter with CO_2 at 25°C	0.0004	d^{-1}
K_{O_2}	Half-saturation coefficient of O_2 in mineralization	0.01[b]	mmol l^{-1}
K_{NO_3}	Half-saturation coefficient of NO_3 in mineralization	0.01[b]	mmol l^{-1}
K_{FeOOH}	Half-saturation coefficient of Fe^{3+} in mineralization	0.3[b]	mmol l^{-1}
$K_{FeOOH,inh}$	Half-saturation inhibition coefficient of Fe^{3+} in mineralization	3[b]	mmol l^{-1}
K_{SO_4}	Half-saturation coefficient of SO_4 in mineralization	0.005[b]	mmol l^{-1}
$K_{SO_4,inh}$	Half-saturation inhibition coefficient of SO_4 in mineralization	0.01[b]	mmol l^{-1}
β_{Oxic}	Temperature-dependent coefficient of aerobic mineralization	0.07[c]	$°C^{-1}$
β_{Anox}	Temperature-dependent coefficient of anaerobic mineralization	0.065[c]	$°C^{-1}$
$k_{FeS,pre}$	Precipitation rate of FeS	$2.5e^{-6}$[b]	mol m^{-3} d^{-1}
$k_{FeS,diss}$	Dissolution rate of FeS	$2.74e^{-6}$[b]	d^{-1}
$k_{Fe_3(PO_4)_2,pre}$	Precipitation rate of $Fe_3(PO_4)_2$	$3e^{-7}$[b]	mol m^{-3} d^{-1}
$k_{Fe_3(PO_4)_2,diss}$	Dissolution rate of $Fe_3(PO_4)_2$	0[b]	d^{-1}
$k_{FeCO_3,pre}$	Precipitation rate of $FeCO_3$	$2.5e^{-5}$[b]	mol m^{-3} d^{-1}
$k_{FeCO_3,diss}$	Dissolution rate of $FeCO_3$	$2.5e^{-7}$[b]	d^{-1}
$k_{CaCO_3,pre}$	Precipitation rate of $CaCO_3$	0.2[b,c]	mol m^{-3} d^{-1}
$k_{CaCO_3,diss}$	Dissolution rate of $CaCO_3$	$2.5e^{-7}$[b,c]	d^{-1}
$\alpha_{H,d}$	Fraction of hydrogen in degradable OM	0.07[b]	
$\alpha_{H,r}$	Fraction of hydrogen in refractory OM	0.07[b]	
$\alpha_{N,d}$	Fraction of nitrogen in degradable OM	0.06	
$\alpha_{N,r}$	Fraction of nitrogen in refractory OM	0.02	
$\alpha_{O,d}$	Fraction of oxygen in degradable OM	0.29	
$\alpha_{O,r}$	Fraction of oxygen in refractory OM	0.29	
$\alpha_{P,d}$	Fraction of phosphorus in degradable OM	0.02	
$\alpha_{P,r}$	Fraction of phosphorus in refractory OM	0.01	
$\alpha_{S,d}$	Fraction of sulfur in degradable OM	0.01[b]	
$\alpha_{S,r}$	Fraction of sulfur in refractory OM	0.01[b]	
$\alpha_{C,d}$	Fraction of carbon in degradable OM	0.55	
$\alpha_{C,r}$	Fraction of carbon in refractory OM	0.6	

[a]Values with no source indication are calibrated from this study.
[b]*Dittrich et al.* [2009].
[c]*Reichert et al.* [2001].

170 mV and a DO concentration of 0.04 mmol l^{-1} in the polluted zone. Such low-oxygen conditions create reducing conditions that convert ions with multiple oxidation states to their reduced form. For iron and manganese, they are more soluble in their reduced (Fe^{2+} and Mn^{2+}, respectively) than in their oxidized state (Fe^{3+} and Mn^{4+}, respectively). Usually, close to the sediment-water interface, redox potential is high enough to convert all reduced metals to oxidized metals, resulting in reprecipitation of Fe and Mn. However, in the polluted zone where redox potential is low in both water and sediment, mobile-dissolved Fe and Mn can move freely from sediment to water thus reducing total Fe and Mn in the sediment and increasing dissolved Fe and Mn in the water column. As the process continues, settling Fe particles decrease in polluted zone compared to the pristine one, which matches the observations. Another notice from experimental results which would be lately used for model setup is that the Fe/Mn ratio in the Day River is very high (average Fe_{tot} and Mn_{tot} are 0.85 and 0.0013 mol kg^{-1}, respectively).

3.1.2. Solute Species Profiles

[29] In general, pore water profiles of solute species demonstrate high rates of organic matter degradation, as determined from the ratio between organic carbon and Kjeldahl nitrogen in the upper few centimeters, near to the sediment-water interface (SWI). These rates then decrease for depths lower than 10 cm (Figure 3). Unsurprisingly, degradation rates are the highest in the polluted sites and the lowest in the pristine sites. Using the pore water concentrations and porosities of the upper most sediment layer and the average surface water concentrations from the monthly surveys, the flux across the water sediment interface is directly calculated following Fick's first law [*Mozeto et al.*, 2001]. This manual calculation shows that there are large differences in the flux of solutes across the sediment-water interface between the three zones (Table 6). For instance, the Alkalinity flux in the polluted zone is almost twice that of the pristine zone and the SRP (PO_4) fluxes in the polluted zone are almost 8 times higher those determined for the pristine zone.

3.2. Simulation Results

[30] The model was constructed following the two-step tactic. In the first step a core model consisting of only diagenetic processes where O_2, NO_3, Fe^{3+}, SO_4, and CO_2 are selected as oxidizers based on their dominance in this river sediment is set up. Degradation by Mn is not used as concentrations are low, usually 50 times less than that of Fe (Table 3). The tuning of the degradation rate coefficients results in a very good fit of the model to the organic matter profiles (Figure 4). These calibrated degradation rate coefficients are listed in Table 5. In the second step the precipitation/dissolution of Calcite ($CaCO_3$), Vivianite ($Fe_3(PO_4)_2$), Pyrite/Troilite (FeS) and Siderite ($FeCO_3$), were integrated

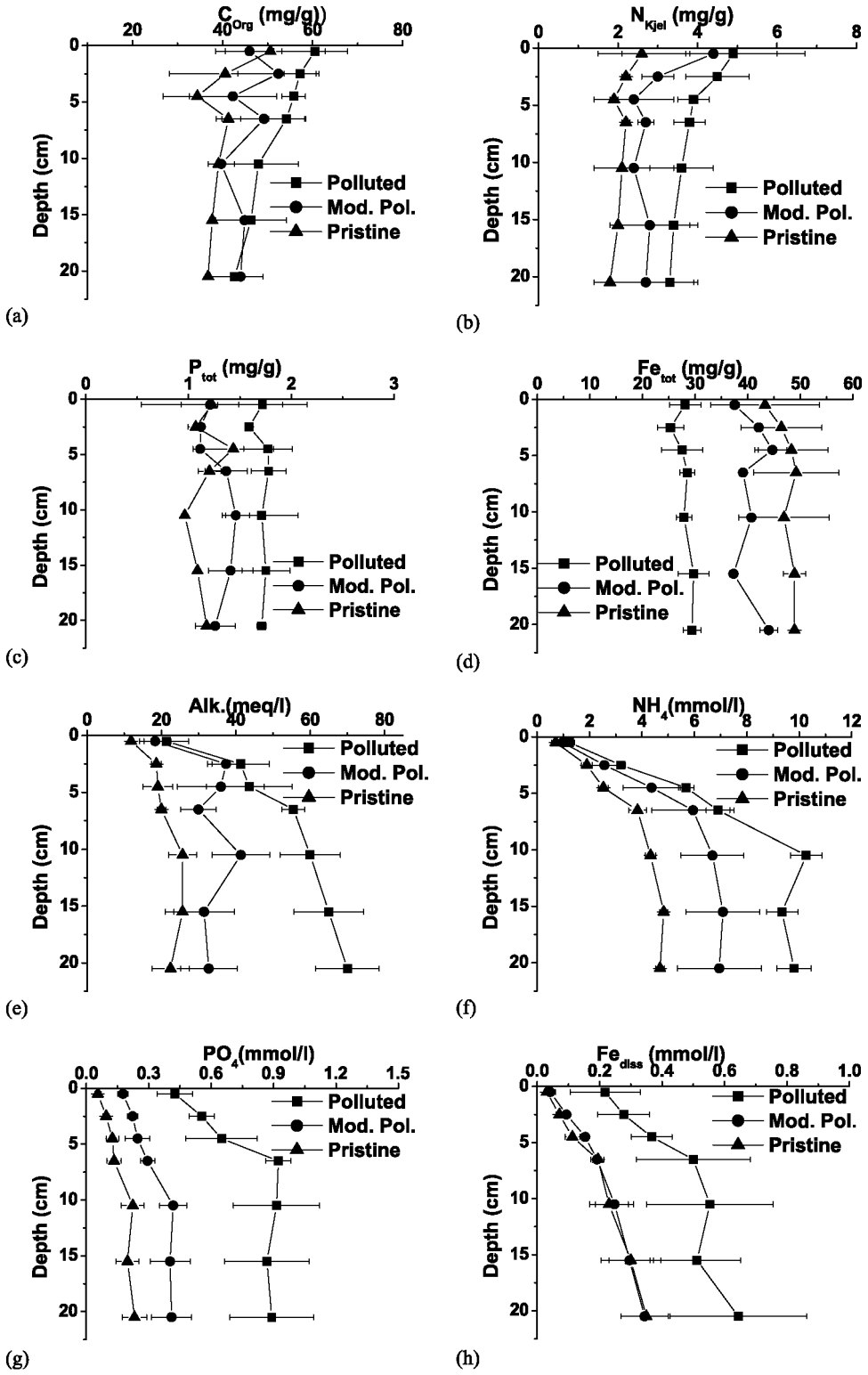

Figure 3. Experimental profiles of sediment cores at different zones: (a–d) solid and (e–h) solute species profiles.

one by one into the model after verification with the geochemical computation program PHREEQC [*Parkhurst and Appelo*, 1999] of the appropriateness of the used geochemical equilibrium reactions. Kinetic parameters of the geochemical reactions are presented in Table 5. To statistically check if the simulation results match the experimental ones, we compare the simulated and analytical sediment profiles using a *t* test for paired data (Microcal Origin version 6). The results (auxiliary material) show that if p value of 0.01 is set as significance level, only Fe_{tot} in pristine zone is found

Table 6. Fluxes of Solute (mol m^{-2} d^{-1}) Calculated Manually and Simulated by Diagenetic Model

	Polluted		Moderately Polluted		Pristine	
	Calculated	Simulated	Calculated	Simulated	Calculated	Simulated
O_2		0.0315				0.0414
Alk	0.1741	0.1043	0.1549	0.0886	0.0941	0.0714
NH_4	0.0139	0.0171	0.0141	0.0134	0.0106	0.0100
NO_3		0.0099		0.0089		0.0074
PO_4	0.0025	0.0015	0.0011	0.0012	0.0003	0.0010

significantly different between simulated and analytical results.[1] A potential explanation for this lower fit lies within the fact that the model only takes into account only some of the complex geochemical processes controlling Fe_{tot}. All other parameters are not significantly different demonstrating the good fit of the simulation results.

[31] Apart from simulating sediment profiles, the diagenetic model calculates the fluxes across the water sediment interface which can then be used to assess the impact of sediment on water quality for the construction of carbon and nutrient budgets. As the modeling is performed in steady state mode, the simulated fluxes are time independent, reflecting the long-term effect of sediment on water column. The simulated fluxes of solutes are shown in Table 6. Of the three parameters (Alk, NH_4, and PO_4) simulated Alkalinity is about 25%–40% smaller than the manually calculated values. Moreover, the model appears to underestimate Alkalinity in the upper sediment layers and overestimate it in the lower sediment layers. This lack of correspondence is potentially a consequence of the high variability of the boundary conditions as determined from the average monthly concentrations. Nevertheless, the two Alk profiles were not significantly different (p values obtained from paired *t* test are 0.48, 0.54, and 0.44 for polluted, moderately polluted, and pristine zones, respectively). The simulated NH_4 fluxes fit well to the manually calculated values within the three zones. On the other hand, the simulated PO_4 fluxes were underestimated in the polluted zone and overestimated in the pristine zones. The underestimations of both Alkalinity and phosphate in the polluted zones may potentially be a consequence of anoxia which may not favor the precipitation of phosphate and carbonate. Unfortunately, due to the lack of data on the chemical composition of the solid phase, dissolution processes involving more complex materials are not modeled. In contrast to the underestimation of PO_4 in the polluted zone, the low value of experimental PO_4 flux in the pristine zone may be due to the association of phosphate with nonmodeled solid materials under high redox potential conditions near the sediment-water interface.

[32] In terms of modeling, the differences between the simulation and experimental fluxes can be due to the high sensitivity of the model outcome to the model parameters. It is possible that small variations in the boundary conditions could lead to significant changes in simulated NH_4 and Alkalinity. Thus a sensitivity analysis focusing on the variability of solute boundary conditions on the model outcome is performed. The model is run with two sets of minimum and maximum solute boundary conditions (Alkalinity, DO, NH_4, NO_3, PO_4, etc.). The ranges of values, taken from the maximum and minimum of the range of variability are established from water quality measurements in the polluted and pristine zones. Comparison of the solute fluxes (auxiliary material) showed that the fluxes of PO_4 and Alkalinity are fairly sensitive (variation of 20%) while flux of NH_4 is not sensitive (variation of only a few percent).

[33] In summary, on the whole, the diagenetic model provides generally realistic results nevertheless, there is still room for improvement, particularly with regards to nonredox geochemical processes.

3.3. Carbon, Nitrogen, and Phosphorus Budgets for the Nhue-Day River System

3.3.1. Mass Balance of Suspended Sediment

[34] One way to validate our approach is to apply it to a mass balance calculation of suspended sediment, the most documented parameter in the study area. In brief, sedimentation load of each area (pristine, moderately polluted, and polluted) is calculated by multiplying the corresponding settling rate by the wetted area (Table 4). The total output of suspended sediment is then determined by subtracting sedimentation load from total input. Figure 5 shows the calculated SS loads exported from the study area to the lower basin area (117 and 783 ton d^{-1} during the dry and rainy seasons, respectively) compared to the value of 410 ton d^{-1} annually reported by *Luu et al.* [2012]. It should be mentioned that the material mass eventually buried into the bottom sediments is smaller than the sedimentation load calculated from the settling rate because of the inverse fluxes of solutes species (e.g., O, H, C, N, P, S, metals) from the sediment to the water column. The latter calculation shows that about 25% of OM settling to the bottom would return to the water column under the dissolved form. Thus total material mass permanently buried into bottom would be about 5% less than number shown in Figure 5. Nevertheless, although this discrepancy should be borne in mind, such a small difference does not have a significant effect on the validity of our approach.

3.3.2. Burial Capacity of C, N, and P

[35] River flow rates are generally low in flat deltaic river systems and most suspended particulates tend to be lost from the water column to the sediments. In this river system, this results in organic rich sediments because of the high OM content in suspended sediment. As represented in Figure 6, during low-water periods up to 124.5 ton d^{-1} of organic matter ends up in sediment. This rate is very high since the inflow of OM at the river boundaries during dry period is only 92.0 ton d^{-1} and implies some other source of OM. Some of this OM production is probably from primary production in the upper water column [*Trinh et al.*, 2006]. Moreover, recent work from the Bach Dang River, part of the Red River system, has shown that rates of water column primary production are up to 0.79 mmol C m^2 h^{-1} in these high-turbidity freshwaters [*Rochelle-Newall et al.*, 2011]. Similarly, OM settling out of the water column during the rainy period is 129.3 ton d^{-1}, representing approximately 51% of the total OM inflow at boundaries. Concomitant with this high OM loading, high rates (17.8 and 18.5 ton C d^{-1} in dry and rainy periods, respectively) of dissolved inorganic carbon (represented as CO_2) release from the sediment are also found (Figure 6).

[1] Auxiliary materials are available at ftp://ftp.agu.org/apend/gb/2010gb003963.

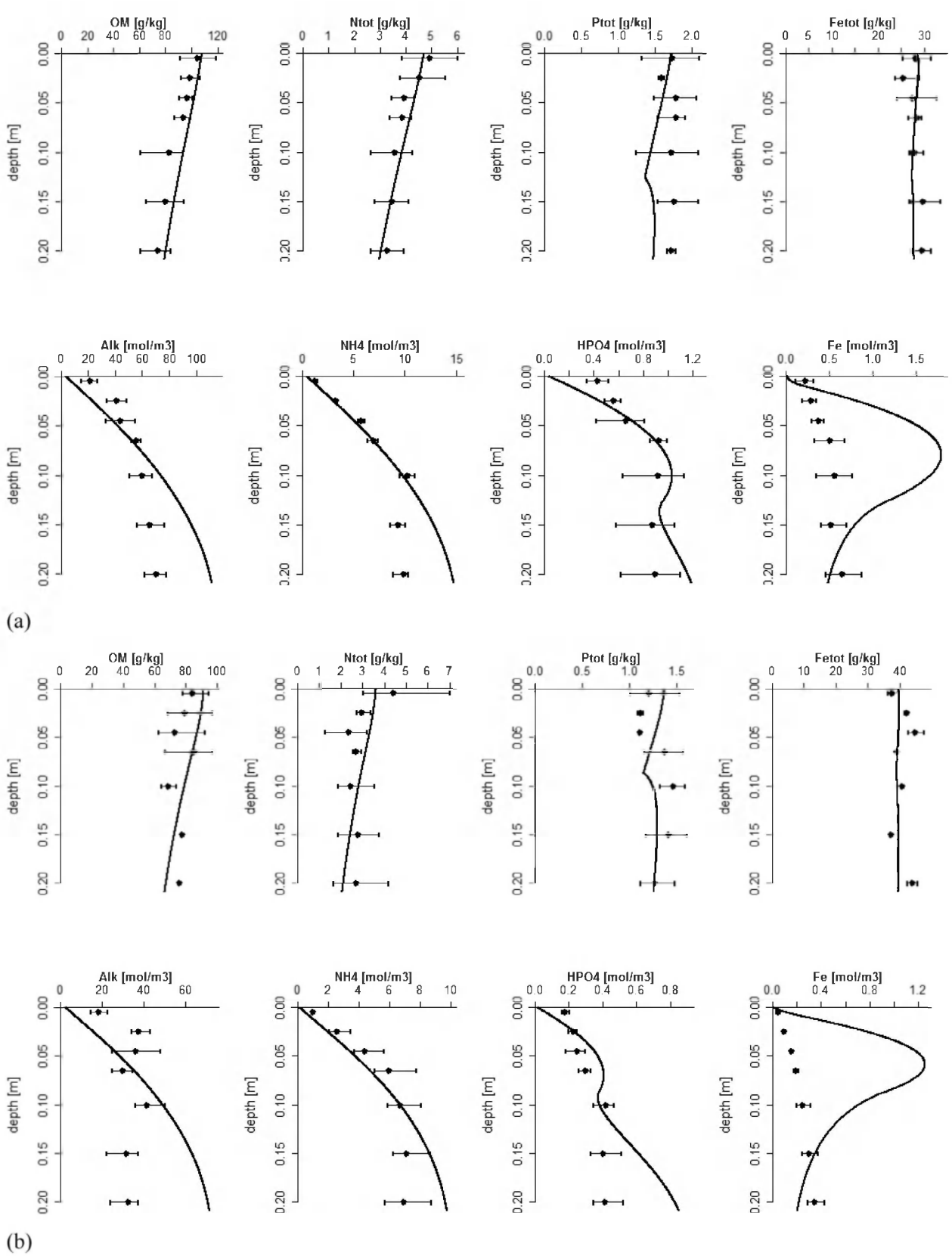

Figure 4. Experimental and simulation profiles from the three zones: (a) polluted, (b) moderately polluted, and (c) pristine.

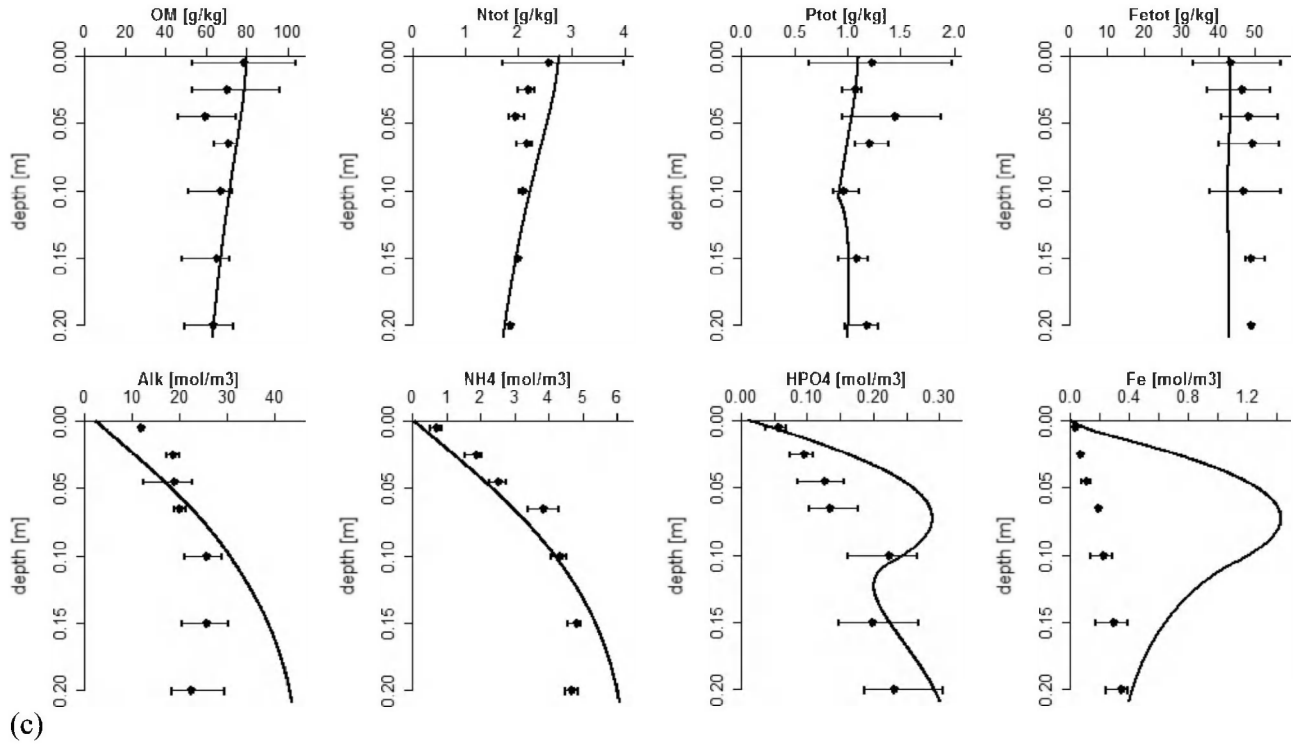

Figure 4. (continued)

According to the simulation results, the amount of C buried in sediment represents 75% of the particulate organic carbon (POC) settling to the bottom. The remaining fraction (17.82 to 18.5 ton d^{-1}, depending on the hydrological regime), returns to water column in the dissolved inorganic form. These high CO_2 efflux (from sediment to water) rates further underline the previous conclusions on the heterotrophic state of the Day River system [*Trinh et al.*, 2009] where low dissolved oxygen concentrations are frequently observed during the monthly surveys. The total load of CO_2 from the water column to the atmosphere as simulated by the hydrodynamic river model of *Trinh et al.* [2006] is 35.6 and 53.01 ton d^{-1} in dry and rainy periods, respectively (Figure 6).

[36] As discussed in the previous subsection, our simulated Alkalinity fluxes effluxing from the sediment are 25%–40% smaller than the manually calculated ones. This is due to the high variability of the boundary conditions calculated from the average monthly concentrations combined with an underestimation of the complex geochemical sedimentary precipitation and dissolution processes. Therefore, if we assume that the manually calculated fluxes are closer to the actual values the efflux from the sediment to water column is between 23 ton d^{-1} and 26 ton d^{-1}. This translates into a C burial of between 65% and 69% of the total amount settling to the bottom.

[37] Similarly, the amount of N eventually buried into the sediment represents up to 81% of the total N settling to the bottom. In other words, the N amount lost from the sediment to the water column is relatively small. *Luu et al.* [2012] reported that the denitrification rates were high (100×10^6 kg N yr^{-1}) in delta region of which this studied river system forms part. This may partly explain the low N efflux from the sediments to the water.

[38] The ratio between the burial of P and the settling of P is 0.68, similar to the burial C:settling C ratio of 0.75. In

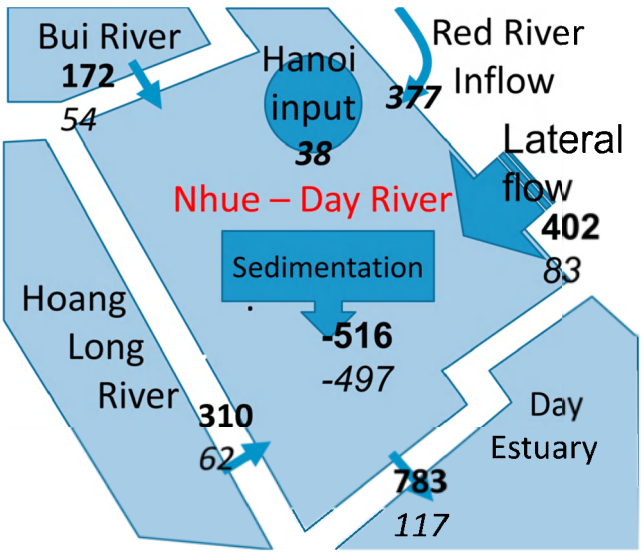

Figure 5. Mass balance of suspended sediment during the rainy season (bold) and dry season (italic). All values are in ton d^{-1}.

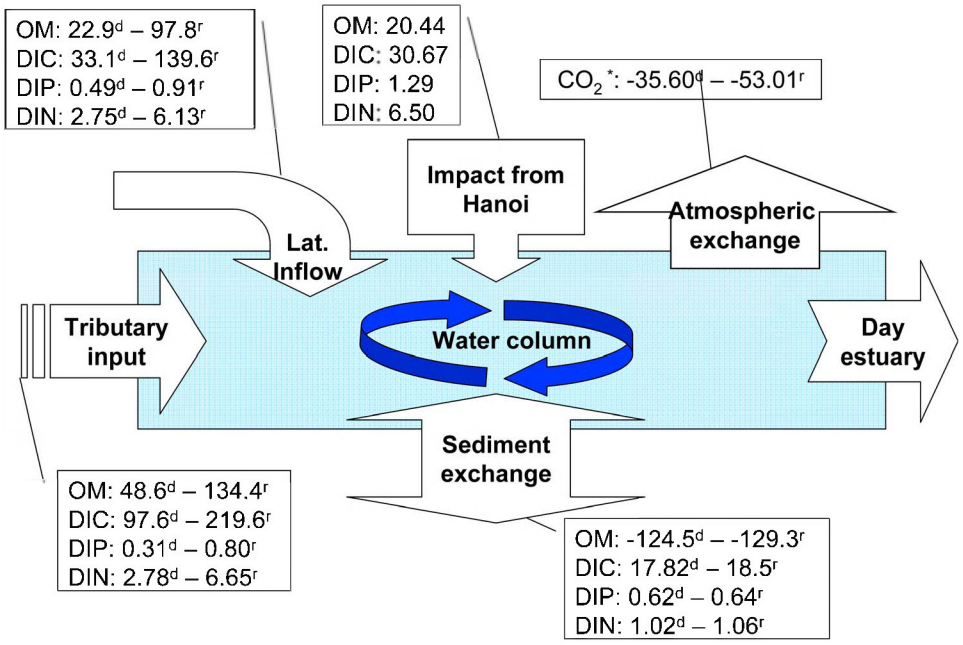

Figure 6. Total inputs and outputs to the study river system (ton d^{-1}) for both seasons. Asterisk values are in ton C d^{-1}. Superscript d denotes the dry season, and superscript r denotes the rainy season.

other words, fraction of PO_4 retained in sediment represents 68% of that arriving at the sediment surface. *Hutchison and Hesterberg* [2004] found that in rich OM environments, precipitation of PO_4 under mineral form is not favorable and this may well explain the case in this system.

3.3.3. Mass Balance of Carbon

[39] Carbon retention within the hydrological network is high (Figure 7). Comparison with data from *Cole et al.* [2007] reveals that fraction of C fraction buried in the Day River system (up to 25% for the dry season) is higher than the globally averaged value (12%). In addition, while on a global scale, carbon stored in sediment is much lower than that lost to atmosphere, in this particular river system, carbon burial in sediment is higher than that lost to atmosphere, in agreement with *Aufdenkampe et al.* [2011]. Thus it appears that sediments play a major role in C storage in deltaic rivers subject to large particulate matter inputs. The mass balance scheme also reveals the impact of the conurbation of Hanoi on OM inputs, since it contributes up to 22% in dry season and 8% in rainy season of total OM input into the system.

[40] It should be noted that in the diagenetic model, only particulate organic matter settles out. This is probably not true as it is known that dissolved organic matter (DOC) can aggregate to form particles that can be important in carbon flux [e.g., *Engel et al.* 2004]. Given that the ratios of DOC: POC are on average 2 in this system, this DOC flux should be taken into account in any future model.

3.3.4. Mass Balance of Nitrogen

[41] In terms of nitrogen dynamics, during the dry season, about 27% of total nitrogen inputs to the hydrological system are retained in the sediments, whereas during the rainy season this value decreases to about 15% (Figure 8). In their approach applied to catchments adjacent to the Nhue-Day River system, *Luu et al.* [2012] and *Le et al.* [2010] calculated the nutrient retention in the hydrological network by subtracting the total load measured at the river mouth from the total input into the catchments. *Luu et al.* [2012] note that N retention of several deltaic catchments in northern Vietnam varied over a large range from 20.7% to 63.5%. *Quynh et al.* [2005] looking at the entire lower Red River basin found N retention to vary from 0.5% to 36%. Results obtained by this type of approach have the disadvantage that it is difficult to use them to identify main factors regulating the water-sediment exchange. In contrast, the deterministic approach presented in this study allows the estimation of the main factors controlling removal process which can then be used to construct future scenarios.

[42] Nitrogen retention calculated by our approach is within the range reported by *Le et al.* [2010] for the

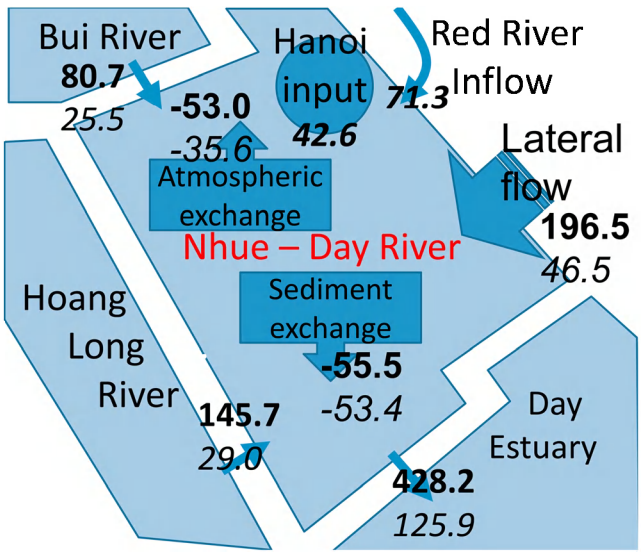

Figure 7. C budget during the dry season (italic) and rainy season (bold). All values are in ton d^{-1}.

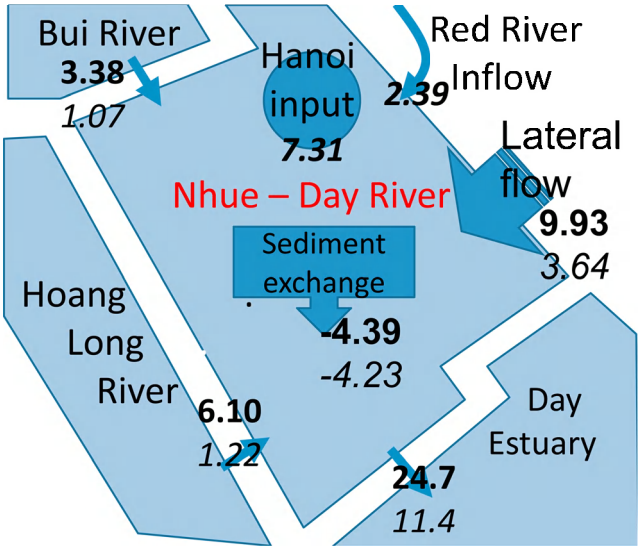

Figure 8. N budget from the dry season (italic) and rainy season (bold). All values are in ton d^{-1}.

subbasins of the Red River system and lower than that reported by *Luu et al.* [2012] for some adjacent deltaic catchments. One explanation for the lower values found here as compared to those of *Luu et al.* [2012] is that their results are based on the calculation of retention within the whole hydrological network (mainstreams, impoundments, reservoirs, canals, and small creeks), whereas our work only looked at the mainstream.

[43] Similar to the carbon budget, the impact of Hanoi on the nitrogen budget is clear. Up to 47% in dry season and 25% in rainy season of total N input into the river system comes from the Hanoi wastewater system. Indeed, these inputs are responsible for the high levels of eutrophication in the "polluted" zone of the Nhue River.

3.3.5. Mass Balance of Phosphorus

[44] Budget calculations for P indicate that 38% of total P inflows are stored in the sediments during the dry period as compared to 20% during the rainy period (Figure 9). These values are smaller than the total P retention of 32.8–88% reported by *Le et al.* [2010] and *Luu et al.* [2012] for the hydrological network of some adjacent catchments. It is interesting to note that the fraction that ends up in the sediment is the highest for the three elements (C, N, and P) examined. This is most probably due to the fact that the relative contribution of the particulate fraction to the total fraction entering into the system is highest among the three elements. For example, ratios of particulate P to dissolved P in the inflow are 1.23 and 0.65 in rainy and dry seasons, respectively. The corresponding values for C are 0.36 and 0.29 and for N are 0.51 and 0.30.

[45] Similar to nitrogen, phosphorus inflow from Hanoi is high, representing 46% and 24% of the total inflow during the dry and rainy season, respectively. These inflows exceed the retention capacity of sediment, as is also the case for nitrogen inflows in this system. In summary, the mass balance schemes presented here show that in the Nhue-Day River system, although large proportions of nutrients and organic matter are potentially buried in sediment, this burial is insufficient to remove the high load of untreated domestic waste from Hanoi city from the water column.

3.3.6. Identification of Limiting Factor

[46] Using the simulation results, we can investigate the potential limiting factor of production in this system. Both *Quynh et al.* [2005] and *Wu et al.* [2003] report that N rather than P is the limiting factor for primary production in the Northern Vietnam riverine and coastal waters. The results of this study also confirm this conclusion. The molar DIN:DIP ratio of inputs to the Nhue River system varies between 12.7 and 14.2 for the dry and rainy periods, respectively. These values are lower than the Redfield ratio of 16, potentially reflecting the wastewater origin of much of the organic matter inputs as the molar DIN:DIP value for wastewater from Hanoi downtown is 11.2. The molar ratio of total N: total P of inflow into the system provides even lower values of 9.6 to 10.0. This is different from the N:P ratio of the sediments, where values of between 4 and 5 are found (Table 3). N:P ratio decreases from inflow to water column and from water to sediment. The preferential loss of P to the sediments rather than N is further supported by the fact that the molar ratio of total N:total P at the outflow of the river system (10.2 and 11.8) is slightly higher than that of the inflow. Nevertheless, despite this preferential loss of P from the system, nitrogen remains the limiting factor.

3.3.7. A Scenario for Treatment of the Hanoi Wastewater

[47] Given the impact of untreated wastewater from the Hanoi area to the Nhue-Day River system, the city is planning to construct a wastewater treatment plant. Here we assess how this treated wastewater could change nutrient inputs to the system. We also reassess the importance of the sediments. For this calculation we assumed that volume discharge from Hanoi remains unchanged after treatment and that water quality post treatment is similar to that of the pristine section. We also assumed that sediment of the whole river system would have the same quality of sediment as in the pristine zone. The results of this simulation are shown in

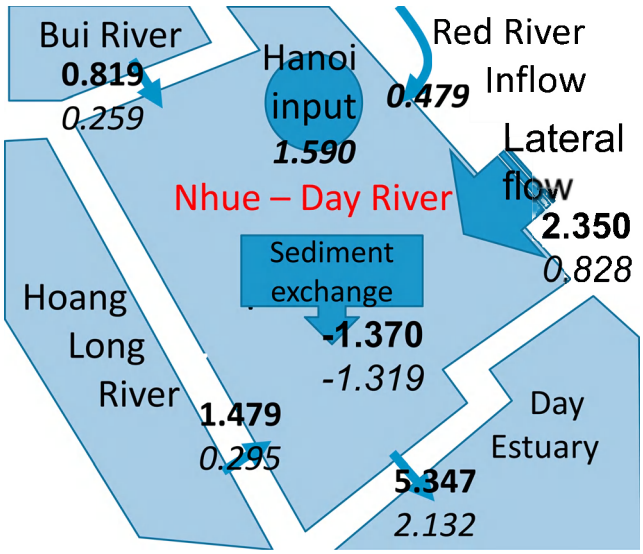

Figure 9. P budget during the dry season (italic) and rainy season (bold). All values are in ton d^{-1}.

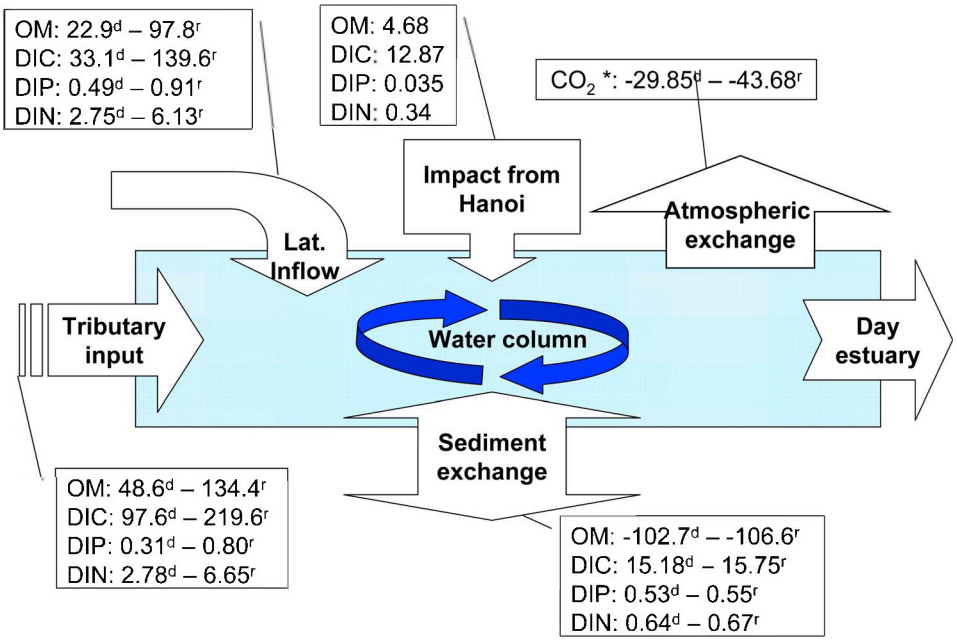

Figure 10. Scenario of treatment of Hanoi wastewater (ton d^{-1}) for both seasons. Asterisk values are in ton C d^{-1}. Superscript d denotes the dry season, and superscript r denotes the rainy season.

Figure 10. As represented in Figure 10, if wastewater from Hanoi were treated to pristine level, its contribution, in terms of C, N, and P, would be trivial and total OM would be reduced from 20.44 to 4.68 ton d^{-1} (77% reduction). Dissolved inorganic carbon would be reduced from 30.67 to 12.87 ton d^{-1}. DIP would be reduced from 1.29 to 0.035 (97%) and DIN would be reduced by 95%. Consequently, the treatment of Hanoi wastewater would reduce 17.51^{d}%–17.56^{r}% of OM currently settling to river bottom (^{d}: dry season, ^{r}: rainy season). Related to the decreased in OM flux, the fluxes of DIC, DIP, and DIN returning to water column will also decrease by 14.81^{d}%–14.86^{r}%, 14.52^{d}%–14.06^{r}%, and 37.25^{d}%–36.79^{r}%, respectively. Thus, over and above a decrease in water sediment exchange, the treatment of Hanoi wastewater may well also decrease the flux of CO_2 to the atmosphere by approximately 17%. In summary, although the discharge of Hanoi wastewater contributes only 4.5%–12% of the total system discharge, wastewater treatment could alleviate approximately 15%, 14%, and 37% of the impact of C, N and P, respectively, to the Nhue-Day River system as well as potentially altering the sedimentation rates in the basin.

4. Conclusion

[48] This work presents the application of a diagenetic model to a case study in Vietnam. The model takes into account the complex biogeochemical processes occurring in the sediments, responding to the need to move forward from the simplified "pipeline versus reactor" view of riverine biogeochemistry as suggested by *Cole et al.* [2007]. The results further underline the importance of understanding the role of sediments in organic carbon cycling, particularly in tropical, urban river systems for which little data presently exist. Moreover, the application of the model to other, similar systems will provide support for management decisions applicable to tropical systems subject to untreated domestic wastewater inputs.

[49] **Acknowledgments.** This paper was written with fruitful support from De Vlaamse Interuniversitaire Raad (VLIR, Belgium), Institute de Recherche pour le Developpement (IRD, France), and the National Foundation for Science and Technology (104.03.45.09, NAFOSTED, Vietnam). Appreciation is sent to Andreas Kleeberg from IGB, Germany; Hojeong Kang from Yonsei University, Korea; Javier Garcia Guinea from MNCN, Spain; and the anonymous reviewers for their invaluable advice and comments.

References

Aufdenkampe, A. K., E. Mayorga, P. A. Raymond, J. M. Melack, S. C. Doney, S. R. Alin, R. E. Aalto, and K. Yoo (2011), Riverine coupling of biogeochemical cycles between land, oceans, and atmosphere, *Frontiers Ecol. Environ.*, *9*, 53–60, doi:10.1890/100014.

Boudreau, B. P. (1996), A method-of-lines code for carbon and nutrient diagenesis in aquatic sediments, *Comput. Geosci.*, *22*, 479–496, doi:10.1016/0098-3004(95)00115-8.

Boulton, A. J., L. Boyero, A. P. Covich, M. Dobson, S. Lake, and R. Pearson (2008), Are tropical streams ecologically different from temperate streams?, in *Tropical Stream Ecology*, edited by D. Dudgeon, pp. 257–284, Elsevier, Amsterdam, doi:10.1016/B978-012088449-0.50011-X.

Clesceri, L. S., A. E. Greenberg, and A. D. Eaton (1999), *Standard Methods for the Examination of Water and Wastewater*, 20th ed., Am. Public Health Assoc., Washington, D. C.

Cleveland, C. C., and D. Liptzin (2007), C:N:P stoichiometry in soil: Is there a "Redfield ratio" for the microbial biomass?, *Biogeochemistry*, *85*, 235–252, doi:10.1007/s10533-007-9132-0.

Cole, J. J., et al. (2007), Plumbing the global carbon cycle: Integrating inland waters into the terrestrial carbon budget, *Ecosystems*, *10*, 172–185, doi:10.1007/s10021-006-9013-8.

Davies, P. M., S. E. Bunn, and S. K. Hamilton (2008), Primary production in tropical streams and rivers, in *Tropical Stream Ecology*, edited by D. Dudgeon, pp. 23–42, Elsevier, Amsterdam, doi:10.1016/B978-012088449-0.50004-2.

Dittrich, M., B. Wehrli, and P. Reichert (2009), Lake sediments during the transient eutrophication period: Reactive-transport model and identifiability study, *Ecol. Modell.*, *220*, 2751–2769, doi:10.1016/j.ecolmodel.2009.07.015.

Dudgeon, D. (2000), The ecology of tropical Asian rivers and streams in relation to biodiversity conservation, *Annu. Rev. Ecol. Syst.*, *31*, 239–263, doi:10.1146/annurev.ecolsys.31.1.239.

Duong, T. T., M. Coste, A. Feurtet-Mazel, D. K. Dang, C. T. Ho, and T. P. Q. Le (2012), Responses and structural recovery of periphytic diatom communities after short-term disturbance in some rivers (Hanoi, Vietnam), *J. Appl. Phycol.*, doi:10.1007/s10811-011-9733-9, in press.

Engel, A., S. Thoms, U. Riebesell, E. Rochelle-Newall, and I. Zondervan (2004), Polysaccharide aggregation as a potential sink of marine dissolved organic carbon, *Nature*, *428*, 929–932, doi:10.1038/nature02453.

Ha, P. Q., M. McLaughlin, and I. Oborn (2006), Nutrient recycling for sustainable agriculture in Viet Nam, in *Improving Plant Nutrient Management for Better Farmer Livelihoods, Food Security and Environmental Sustainability*, *Pap. 12*, pp. 158–165, Food and Agric. Organ., Bangkok, Thailand.

Hutchison, K. J., and D. Hesterberg (2004), Dissolution of phosphate in a phosphorus-enriched ultisol as affected by microbial reduction, *J Environ. Qual.*, *33*(5), 1793–1802, doi:10.2134/jeq2004.1793.

Jacobsen, D., C. Cressa, J. M. Mathooko, and D. Dudgeon (2008), Macroinvertebrates: Composition, life histories and production, in *Tropical Stream Ecology*, edited by D. Dudgeon, pp. 65–105, Elsevier, Amsterdam, doi:10.1016/B978-012088449-0.50006-6.

Katsev, S., D. G. Rancourt, and I. L'Heureux (2004), dSED: A database tool for modeling sediment early diagenesis, *Comput. Geosci.*, *30*, 959–967, doi:10.1016/j.cageo.2004.06.005.

Khai, N. M. (2007), Effects of using wastewater and biosolids as nutrient sources on accumulation and behaviour of trace metals in Vietnamese soils, PhD dissertation, 71 pp., Swedish Univ. of Agric. Sci., Uppsala.

Le, T. P. Q., B. Gilles, J. Garnier, T. Sylvain, R. Denis, N. X. Anh, and C. V. Minh (2010), Nutrient (N, P, Si) transfers in the subtropical Red River system (China and Vietnam): Modelling and budget of nutrient sources and sinks, *J. Asian Earth Sci.*, *37*(3), 259–274, doi:10.1016/j.jseaes.2009.08.010.

Lewandowski, J., and M. Hupfer (2005), Effect of macrozoobenthos on two-dimensional small-scale heterogeneity of pore water phosphorus concentrations in lake sediments: A laboratory study, *Limnol. Oceanogr.*, *50*(4), 1106–1118, doi:10.4319/lo.2005.50.4.1106.

Lewis, W. M., Jr. (2008), Physical and chemical features of tropical flowing waters, in *Tropical Stream Ecology*, edited by D. Dudgeon, pp. 1–21, Elsevier, Amsterdam.

Luu, T. N. M., J. Garnier, G. Billen, D. Orange, J. Némery, T. P. Q. Le, H. T. Tran, and L. A. Le, (2010), Hydrological regime and water budget of the Red River Delta (northern Vietnam), *J. Asian Earth Sci.*, *37*, 219–228.

Luu, T. N. M., J. Garnier, G. Billen, T. P. Q. Le, J. Nemery, D. Orange, and L. A. Le (2012), N, P, Si budgets for the Red River Delta (northern Vietnam): How the delta affects river nutrient delivery to the sea, *Biogeochemistry*, *107*, 241–259, doi:10.1007/s10533-010-9549-8.

Meysman, F. (2001), MEDIA: An object-oriented problem-solving environment for early diagenetic problems, in *Modelling the Influence of Ecological Interactions on Reactive Transport Processes in Sediments*, pp. 143–185, Netherlands Inst. of Ecol., Yerseke.

Morel, F. M. M., and J. G. Hering (1993), *Principles and Application of Aquatic Chemistry*, Wiley, New York.

Mozeto, A. A., P. F. Silvério, and A. Soares (2001), Estimates of benthic fluxes of nutrients across the sediment-water interface (Guarapiranga reservoir, São Paulo, Brazil), *Sci. Total Environ.*, *266*, 135–142, doi:10.1016/S0048-9697(00)00726-9.

Parkhurst, D. L., and C. A. J. Appelo (1999), User's guide to PHREEQC (version 2)–A computer program for speciation, batch-reaction, one-dimensional transport, and inverse geochemical calculations, *Water Resour. Invest. Rep. 99–4259*, 312 pp., U.S. Geol. Surv., Denver, Colo.

Pringle, C. M., F. N. Scatena, P. Paaby-Hansen, and M. Nuñez-Ferrera (2000), River conservation in Latin America and the Caribbean, in *Global Perspectives on River Conservation: Science, Policy, and Practice*, edited by P. J. Boon, B. R. Davies, and G. E. Petts, pp. 41–77, John Wiley, Chichester, U. K.

Quynh, L. T. P., G. Billen, J. Garnier, S. Théry, C. Fézard, and C. V. Minh (2005), Nutrient (N, P) budgets for the Red River basin (Vietnam and China), *Global Biogeochem. Cycles*, *19*, GB2022, doi:10.1029/2004GB002405.

Reichert, P., D. Borchardt, M. Henze, W. Rauch, P. Shanahan, L. Somlyódy, and P. Vanrolleghem (2001), River water quality model no. 1 (RWQM1): II. Biochemical process equations, *Water Sci. Technol.*, *43*(5), 11–30.

Rochelle-Newall, E. J., et al. (2011), Phytoplankton distribution and productivity in a highly turbid, tropical coastal system (Bach Dang Estuary, Vietnam), *Mar. Pollut. Bull.*, *62*, 2317–2329, doi:10.1016/j.marpolbul.2011.08.044.

Soetaert, K., and F. Meysman (2011), Reactive transport modelling in 1D, 2D and 3D, version 1.3.2., The R Found. for Stat. Comput., Vienna.

Soetaert, K., P. M. J. Herman, and J. J. Middelburg (1996), A model of early diagenetic processes from the shelf to abyssal depths, *Geochim. Cosmochim. Acta*, *60*, 1019–1040, doi:10.1016/0016-7037(96)00013-0.

Soetaert, K., T. Petzoldt, and R. W. Setzer (2010), Solving differential equations in R: Package deSolve, *J. Stat. Software*, *33*(9), 1–25.

Trinh, A. D., M. P. Bonnet, G. Vachaud, C. V. Minh, N. Prieur, L. V. Duc, and L. L. Anh (2006), Biochemical modeling of the Nhue River (Hanoi, Vietnam): Practical identifiability analysis and parameters estimation, *Ecol. Modell.*, *193*, 182–204, doi:10.1016/j.ecolmodel.2005.08.029.

Trinh, A. D., G. Vachaud, M. P. Bonnet, N. Prieur, V. D. Loi, and L. L. Anh (2007), Experimental investigation and modelling approach of the impact of urban wastewater on a tropical river; a case study of the Nhue River, Hanoi, Viet Nam, *J Hydrol.*, *334*, 347–358, doi:10.1016/j.jhydrol.2006.10.022.

Trinh, A. D., N. H. Giang, G. Vachaud, and S.-U. Choi (2009), Application of excess carbon dioxide partial pressure ($EpCO_2$) to the assessment of trophic state of surface water in the Red River Delta of Vietnam, *Int. J. Environ. Stud.*, *66*(1), 27–47, doi:10.1080/00207230902760473.

Tromp, T. K., P. Van Cappellen, and R. M. Key (1995), A global model for the early diagenesis of organic carbon and organic phosphorus in marine sediments, *Geochim. Cosmochim. Acta*, *59*, 1259–1284, doi:10.1016/0016-7037(95)00042-X.

Tue, N. T., H. Hamaoka, A. Sogabe, T. D. Quy, M. T. Nhuan, and K. Omori (2011), The application of $\delta^{13}C$ and C/N ratios as indicators of organic carbon sources and paleoenvironmental change of the mangrove ecosystem from Ba Lat Estuary, Red River, Vietnam, *Environ. Earth Sci.*, *64*(5), 1475–1486, doi:10.1007/s12665-011-0970-7.

Van Cappellen, P., and Y. Wang (1996), Cycling of iron and manganese in surface sediments: A general theory for the coupled transport and reaction of carbon, oxygen, nitrogen, sulfur, iron and manganese, *Am. J Sci.*, *296*, 197–243, doi:10.2475/ajs.296.3.197.

van den Bergh, G. D., W. Boer, M. A. S. Schaapveld, D. M. Duc, and T. C. E. van Weering (2007), Recent sedimentation and sediment accumulation rates of the Ba Lat prodelta (Red River, Vietnam), *J Asian Earth Sci.*, *29*(4), 545–557, doi:10.1016/j.jseaes.2006.03.006.

Walkley, A., and I. A. Black (1934), An examination of Degtjareff method for determining soil organic matter and a proposed modification of the chromic acid titration method, *Soil Sci.*, *37*, 29–37.

Winemiller, K. O., A. A. Agostinho, and É. P. Caramaschi (2008), Fish ecology in tropical streams, in *Tropical Stream Ecology*, edited by D. Dudgeon, pp. 107–146, Elsevier, Amsterdam, doi:10.1016/B978-012088449-0.50007-8.

Wishart, M. J., B. R. Davies, P. J. Boon, and C. M. Pringle (2000), Global disparities in river conservation: "First world" values and "third world" realities, in *Global Perspectives on River Conservation: Science, Policy, and Practice*, edited by P. J. Boon, B. R. Davies, and G. E. Petts, pp. 353–369, John Wiley, Chichester, U. K.

Wu, J., S.-W. Chung, L.-S. Wen, K.-K. Liu, Y. L. Chen, H.-Y. Chen, and D. M. Karl (2003), Dissolved inorganic phosphorus, dissolved iron, and *Trichodesmium* in the oligotrophic South China Sea, *Global Biogeochem. Cycles*, *17*(1), 1008, doi:10.1029/2002GB001924.